

Coupling between marine boundary layer clouds and summer-to-summer sea surface temperature variability over the North Atlantic and Pacific

Timothy A. Myers¹  · Carlos R. Mechoso¹ · Michael J. DeFlorio²

Received: 28 September 2016 / Accepted: 16 March 2017 / Published online: 1 April 2017
© Springer-Verlag Berlin Heidelberg 2017

Abstract Climate modes of variability over the Atlantic and Pacific may be amplified by a positive feedback between sea-surface temperature (SST) and marine boundary layer clouds. However, it is well known that climate models poorly simulate this feedback. Does this deficiency contribute to model-to-model differences in the representation of climate modes of variability? Over both the North Atlantic and Pacific, typical summertime interannual to interdecadal SST variability exhibits horseshoe-like patterns of co-located anomalies of shortwave cloud radiative effect (CRE), low-level cloud fraction, SST, and estimated inversion strength over the subtropics and midlatitudes that are consistent with a positive cloud feedback. During winter over the midlatitudes, this feedback appears to be diminished. Models participating in the Coupled Model Intercomparison Project phase 5 that simulate a weak feedback between subtropical SST and shortwave CRE produce smaller and less realistic amplitudes of summertime SST and CRE variability over the northern oceans compared to models with a stronger feedback. The change in SST amplitude per unit change in CRE amplitude among the models and observations may be understood as the temperature response of the ocean mixed layer to a unit change

in radiative flux over the course of a season. These results highlight the importance of boundary layer clouds in interannual to interdecadal atmosphere–ocean variability over the northern oceans during summer. The results also suggest that deficiencies in the simulation of these clouds in coupled climate models contribute to underestimation in their simulation of summer-to-summer SST variability.

Keywords Clouds · Marine boundary layer · Climate variability · Sea surface temperature · Climate models

1 Introduction

The observational record and idealized modeling studies suggest that low-level clouds over the eastern subtropical oceans can amplify modes of climate variability found over the Atlantic and Pacific via their strong coupling to sea-surface temperature (Norris et al. 1998; Tanimoto and Xie 2002; Cassou et al. 2004; Burgman et al. 2008; Clement et al. 2009; Evan et al. 2013; Bellomo et al. 2014, 2015, 2016; Brown et al. 2016; Yuan et al. 2016). Through the modification of boundary layer processes, an increase in sea-surface temperature (SST) over the subtropics causes a decrease in cloudiness, which itself promotes warmer SST by increasing the amount of solar radiation reaching the ocean surface (Bretherton 2015 and references therein). In fact, just a 1% absolute decrease in subtropical cloud fraction increases the solar radiation directed toward the surface by $\sim 1 \text{ W m}^{-2}$ (Klein and Hartmann 1993). Conversely, a decrease in SST causes an increase in cloudiness, which then promotes colder SST. Subtropical clouds and SST are thus linked by a positive feedback loop. Such a feedback may sustain and enhance SST anomalies over the subtropics by reducing their inherent damping by sensible and

Electronic supplementary material The online version of this article (doi:10.1007/s00382-017-3651-8) contains supplementary material, which is available to authorized users.

✉ Timothy A. Myers
tamyers@ucla.edu

¹ Department of Atmospheric and Oceanic Sciences, University of California, 520 Portola Plaza, 7127 Math Sciences Building, Los Angeles, CA 90095, USA

² Jet Propulsion Laboratory, California Institute of Technology, Pasadena, CA, USA

latent heat flux, thereby amplifying the subtropical signature of modes of climate variability characterized by coherent, basin-wide anomalies of SST. Given that the relationship between subtropical clouds and SST is so disparate among climate models (Bony and Dufresne 2005; Clement et al. 2009; Qu et al. 2014; Myers and Norris 2015), it is reasonable to ask: Is this disparity related to model-to-model differences in the representation of climate modes of variability? This is a central question of the present study.

If low-level clouds indeed act to amplify modes of climate variability, anomalously warm SST associated with some mode ought to spatially co-occur with anomalously reduced cloudiness, and cold SST ought to co-occur with enhanced cloudiness. Such a correlation has been detected in observations between the dominant mode of North Pacific SST variability and cloud fraction over both subtropical and midlatitude low-level cloud regions where optically thick stratus and stratocumulus clouds are prevalent (Norris et al. 1998; Burgman et al. 2008; Clement et al. 2009). North Pacific SST varies most strongly on interannual and interdecadal timescales, and the coherent basin-wide spatial pattern of this low-frequency variability is often referred to as the Pacific Decadal Oscillation (PDO; e.g. Mantua et al. 1997). Similarly, Tanimoto and Xie (2002) found a spatially coherent relationship over the northern and southern subtropical Atlantic between SST and low-level cloud fraction anomalies associated with a mode of climate variability characterized by a SST dipole between the North and South Atlantic, which they referred to as the Pan Atlantic Decadal Oscillation. Using independent cloud datasets, Bellomo et al. (2016) and Yuan et al. (2016) found that low clouds vary in a manner consistent with their acting as a positive feedback on the tropical branch of the Atlantic Multidecadal Oscillation (AMO)—the dominant mode of climate variability over the North Atlantic.

A slew of recent studies have used idealized models to provide causal evidence for the role of low clouds in the amplification of unforced modes of climate variability. Evan et al. (2013) built an analytical linear model of atmosphere–ocean coupling over the Atlantic. Based on observational constraints, they found that low clouds act as a positive feedback on subtropical SST anomalies north and south of the equator by increasing the time-scale of Newtonian cooling. Bellomo et al. (2015) artificially increased the strength of the relationship between cloud-induced radiative flux anomalies and SST over the subtropical southeast Atlantic in an atmospheric model coupled to a slab ocean. The result was an enhanced amplitude and persistence of the Atlantic Niño on the interdecadal timescale. In a similar study, Bellomo et al. (2014) found that increasing the strength of the cloud-SST feedback over the subtropical southeast Pacific in the

same model resulted in enhanced amplitude and persistence of interdecadal El Niño variability, and that amplifying the feedback over the subtropical northeast Pacific led to greater PDO-like variability. Lastly, by comparing simulations in a fully coupled model with and without interactive clouds, Brown et al. (2016) found that low clouds over the North Atlantic enhance the amplitude of SST variability throughout the basin, particularly over the midlatitudes, and that these clouds are necessary to produce the AMO.

Is there a distinction in basin-wide cloud-SST coupling from one season to the next? During winter over the northern oceans, interannual to interdecadal sea-level pressure (SLP) variability is strong and forces changes in SST via the alteration of sensible and latent heat fluxes by surface winds, while low-level cloud fraction variability over the North Pacific is weak (Cayan 1992; Deser and Blackmon 1993; Norris et al. 1998; Saravanan 1998; Alexander 2010; Fan and Schneider 2012). In contrast, during summer over the North Pacific, interannual to interdecadal SLP variability is weak, yet changes in SST are of comparable magnitude as in winter and coherently related to basin-wide anomalies of low-level cloud fraction (Norris et al. 1998; Wang et al. 2012). The ocean mixed layer is also shallower in summer than in winter, making SST more sensitive to perturbations in radiative flux at the surface. Norris et al. (1998) therefore speculated that a positive cloud feedback may drive the persistence of SST anomalies associated with the dominant mode of North Pacific SST variability in summer. The question of whether such a seasonal contrast in cloud effects occurs over the North Atlantic as well remains open. In sum, idealized modeling studies suggest that unforced interannual to interdecadal fluctuations in SST in different oceans basins are amplified by a strong low cloud-SST feedback, and observations are physically consistent with this notion.

In the present study, we provide new evidence for a linkage between the cloud-SST feedback and the dominant modes of climate variability over both the North Atlantic and Pacific in both observations and across 19 models participating in the Coupled Model Intercomparison Project phase 5 (CMIP5; Taylor et al. 2012). Our key aim is to determine whether climate models that more realistically capture cloud-SST feedback strength simulate more realistic basin-scale patterns of SST associated with the dominant modes. We consider summer and winter separately in order to allow for an interseasonal and interbasin assessment of cloud-SST modes. Our findings improve the understanding of how modes of climate variability operate in nature and highlight the challenges associated with their successful simulation in global climate models.

2 Data and methods

A useful parameter for diagnosing clouds' impact on SST is cloud radiative effect (CRE). In the present study, CRE is defined as outgoing shortwave (SW) radiation during clear-sky conditions minus outgoing radiation during all-sky (clear plus cloudy) conditions at the top of the atmosphere (TOA). Monthly mean CRE is provided by the International Satellite Cloud Climatology Project (ISCCP) for the years 1985–2000 and Clouds and Earth's Radiant Energy System (CERES) Energy Balanced and Filled dataset version 2.8 for 2001–2014 (Zhang et al. 2004; Loeb et al. 2009). ISCCP CRE was corrected for artifacts as in Norris and Evan (2015), although the results were found insensitive to using uncorrected data. Using CRE provided by two independent satellite datasets from non-overlapping periods allows us to assess the robustness of the results. We have verified that the results are very similar using 1985–2009 ISCCP data. TOA CRE rather than surface CRE is primarily examined because the former is more reliable than the latter in observations (Stephens et al. 2012). Nevertheless, we note that the results are very similar for surface SW and net CRE, as discussed in Sect. 3.

In order to assess which cloud types contribute most to CRE variability in the observational record, we also examine monthly mean cloud fraction (CF) from ISCCP (1985–2000; Rossow and Schiffer 1999) and CERES (2001–2014). The CERES product used is the ISCCP-D2like-Mrg dataset, which is based on daytime retrievals from the Moderate Resolution Imaging Spectroradiometer (MODIS) and geostationary satellites (Sun et al. 2010). ISCCP CF was corrected for artifacts as in Norris and Evan (2015). Each dataset provides CF separated according to cloud-top pressure, including vertically low- (1000–680 hPa), mid- (680–440 hPa), and high-level (440–10 hPa) categories. ISCCP sometimes misplaces actual low-level clouds in the mid-level category over boundary layer cloud regions where strong temperature inversions exist (Garay et al. 2008). In view of our particular interest in these regions, we add low- and mid-level CF together to attain a more accurate estimate of actual low-level values. The same method is applied to the CERES data. The resulting quantity, low+mid-level CF, is considered to be a more reliable measure of boundary layer CF than unadjusted low-level CF provided by the satellite datasets.

Monthly mean SST, near-surface horizontal wind velocity, and SLP for 1985–2014 are obtained from the Interim European Centre for Medium-Range Weather Forecasts (ECMWF) re-analysis (ERA-Interim; Dee et al. 2011). We have verified that the results are virtually unchanged when we use SST from the National Oceanic and Atmospheric Administration (NOAA) Optimum Interpolation

SST dataset V2 (Reynolds et al. 2002) instead of that from the reanalysis. From ERA-Interim we also obtain other large-scale meteorological factors related to boundary layer cloudiness (see e.g. Wood 2012; Bretherton 2015 and; Myers and Norris 2015 for an overview of how these factors are related to MBL cloudiness): estimated inversion strength (EIS, Wood and Bretherton 2006), horizontal surface temperature advection over the SST gradient (SSTadv), relative humidity at 500 hPa (RH_{500}), and pressure vertical velocity at 500 hPa (ω_{500}). EIS and SSTadv are computed as described in Myers and Norris (2015).

We partition our results into summer and winter seasons. Three-month seasonal averages of each climate field for each year are computed during June–July–August (JJA) and December–January–February (DJF). Then, for each season and separate time period corresponding to the non-overlapping ISCCP and CERES records, the averages are linearly detrended to yield interannual anomalies. Note that detrending the raw seasonal averages is equivalent to removing their long-term mean and then detrending.

From single realizations of 1976–2005 historical runs of 19 CMIP5 models, we examine monthly mean SW CRE, SST, near-surface winds, and SLP (Table S1). The period of record was chosen to match that corresponding to observations as closely as possible, including the number of years. For each modeling group we only include model variants with different oceanic or atmospheric components, since our interest is on the model-to-model differences in climate modes of variability, which we do not expect to be significantly affected by different land models or resolutions. We compute JJA and DJF seasonal averages of all climate fields and linearly detrend these averages for 1976–2005 to obtain interannual anomalies. This roughly removes the effect of increasing greenhouse gases in the model simulations. To facilitate ensemble averaging and intercomparison, all observational and CMIP5 fields were bi-linearly interpolated to an equal-angle $2.5^\circ \times 2.5^\circ$ grid prior to analysis.

3 Results

3.1 Observational evidence for positive cloud feedback over northern oceans during summer

The left panels of Figs. 1 and 2 display the slopes of the linear regression of JJA SW CRE, SST, SLP, and surface wind anomalies onto the 1985–2014 normalized time series of JJA SST anomalies averaged over the regions of maximum stratiform cloud amount in the subtropical northeast (NE) Atlantic and subtropical NE Pacific, respectively. These regions are taken from Klein and Hartmann 1993, and outlined with black rectangles in the figures. Nearly

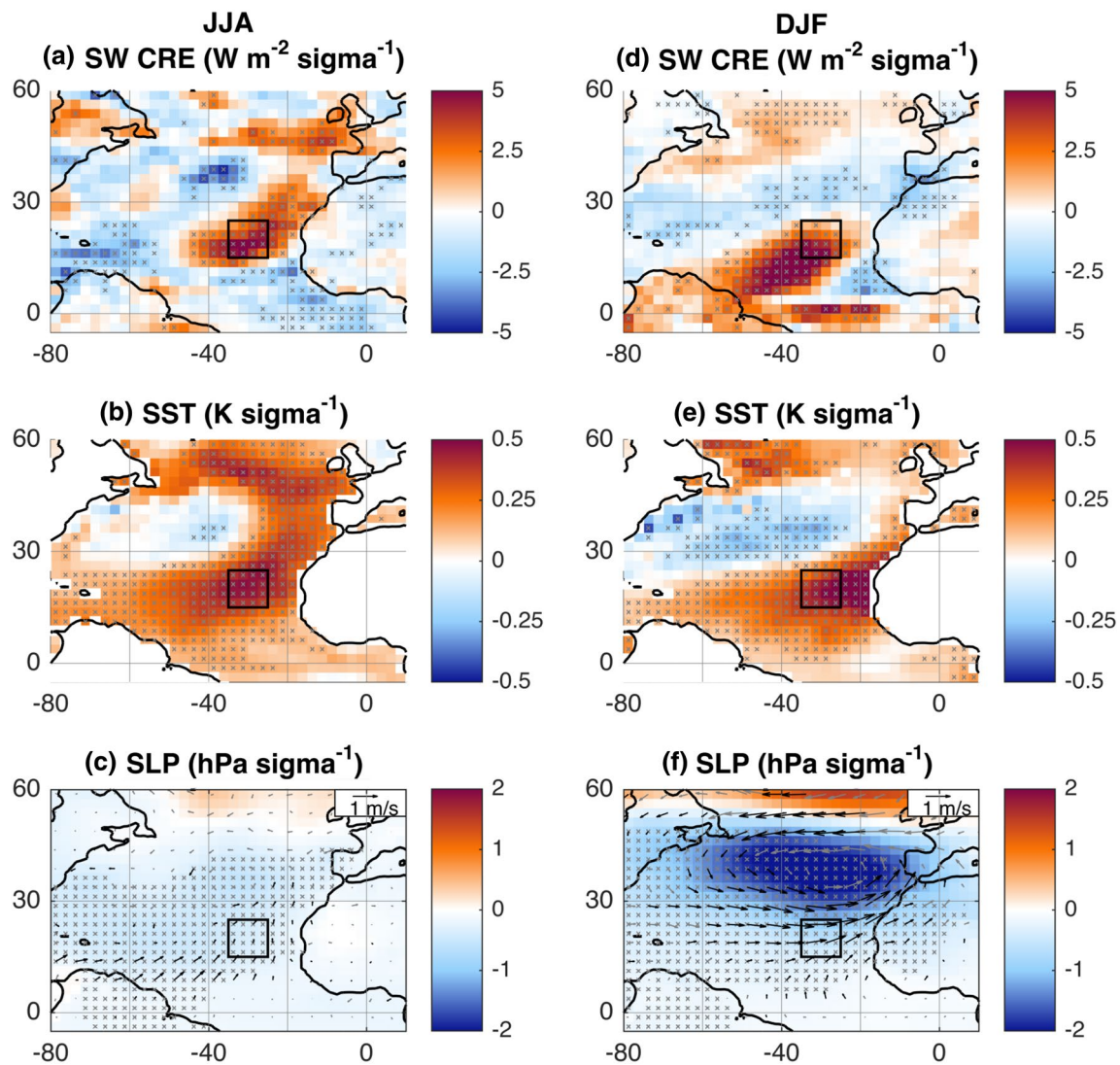


Fig. 1 Slopes of regression of JJA **a** SW CRE at TOA, **b** SST, and **c** SLP and surface wind anomalies onto the 1985–2014 normalized time series of JJA SST anomalies averaged over the subtropical NE Atlantic based on observations provided by ISCCP, CERES, and the ERA-Interim reanalysis. The time series of anomalies are created here and for subsequent observational results by merging together anomalies from the separate 1985–2000 and 2001–2014 records,

respectively. **d–f** are as in **a–c** but for DJF. X's indicate statistical significance at the 95% confidence level using a two-tailed *t* test, taking into account temporal autocorrelation. *Black wind vectors* indicate statistical significance of either the *u* or *v* component of the wind. The region over which SST is averaged to create the time series is shown as a *black rectangle*

identical patterns emerge when the climate fields are regressed onto the normalized time series of the first principal component (PC) of the empirical orthogonal function (EOF) of North Atlantic (10–60°N, 80–0°W) or Pacific (10–60°N, 120–260°E) JJA SST anomalies, each of which exhibits substantial interannual and interdecadal variability. This is evidence that the regression patterns are associated with the dominant modes of summertime SST variability over the northern oceans. During summer over each ocean basin, a horseshoe-like pattern of statistically significant SW CRE (Figs. 1a, 2a) and SST (Figs. 1b, 2b) anomalies is evident. In particular, a standard deviation increase in SST

over the subtropical NE Atlantic is associated with a pattern that resembles the warm phase of the AMO (Bellomo et al. 2016). Additionally, a standard deviation increase in SST over the subtropical NE Pacific is associated with a pattern that resembles the warm phase of the PDO (Mantua et al. 1997). For each pattern of variability, warm (cold) SST anomalies in the subtropics and midlatitudes generally co-occur with positive (negative) SW CRE anomalies, consistent with clouds' acting as a positive feedback on SST and in agreement with previous observational studies (Norris et al. 1998; Tanimoto and Xie 2002; Cassou et al. 2004; Burgman et al. 2008; Clement et al. 2009; Bellomo et al.

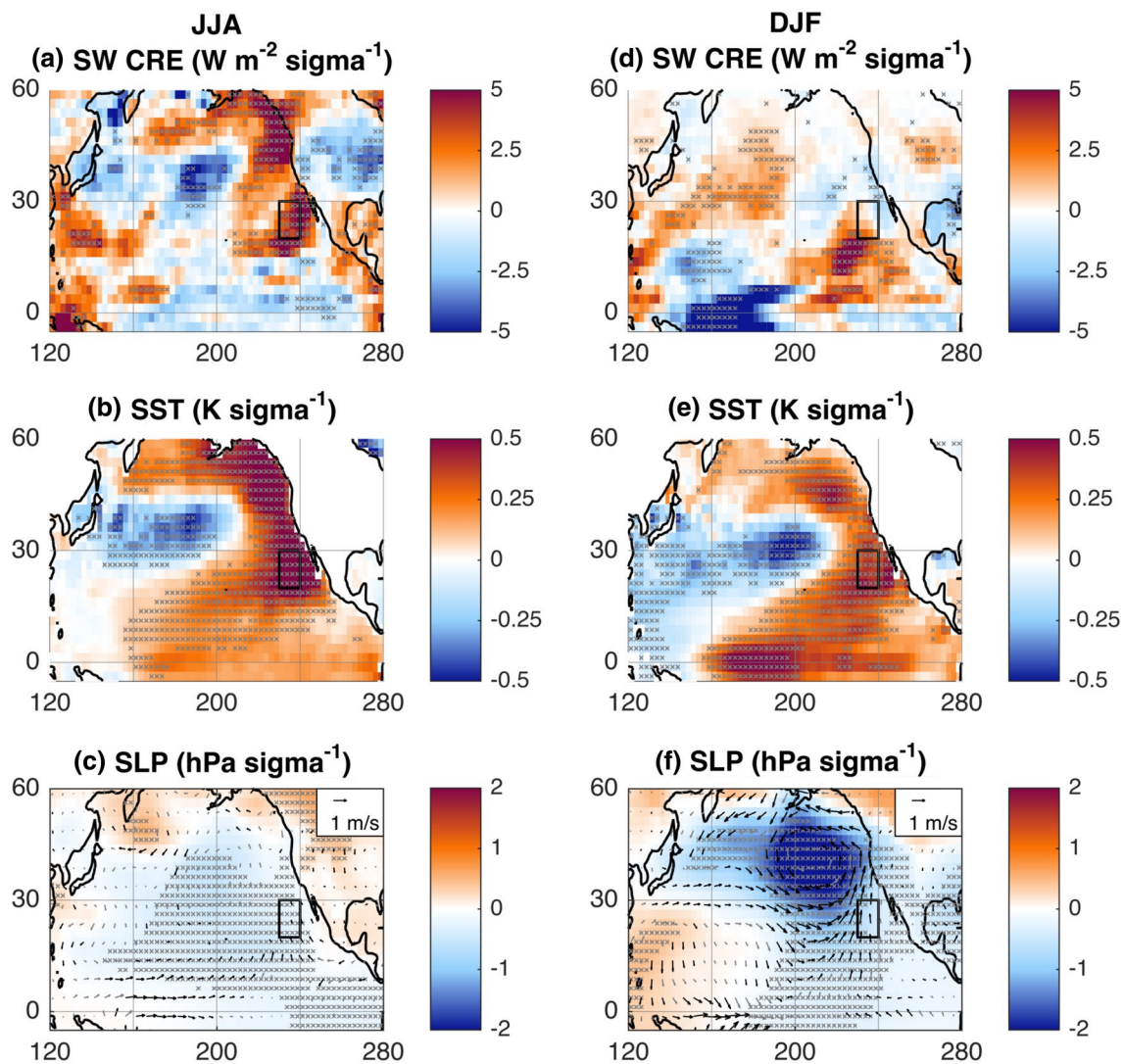


Fig. 2 As in Fig. 1 but for the subtropical NE Pacific

2016; Yuan et al. 2016). The regression patterns obtained using surface SW CRE, longwave (LW) CRE, net CRE, low + mid-level CF, high-level CF, and total CF show that the horseshoe patterns of TOA SW CRE anomalies seen in Figs. 1a and 2a also emerge in the surface net CRE, low + mid-level CF, and total CF anomalies (Figs. S1–S4). Hence, the TOA SW CRE anomaly pattern is representative of basin-scale changes in marine boundary layer (MBL) clouds and surface radiative flux, with the contribution from high clouds of second order. The magnitudes of SLP and surface wind anomalies associated with the horseshoe patterns of SST variability (Figs. 1c, 2c) are very small.

To investigate the possible role of other cloud-controlling factors besides SST in shaping the pattern of SW CRE anomalies seen in Figs. 1a and 2a, we show in the left panels of Figs. 3 and 4 the slopes of the regression of EIS, SSTadv, RH₅₀₀, and ω_{500} onto subtropical NE Atlantic and

Pacific SST during summer. The EIS anomalies associated with a standard deviation increase in subtropical NE Atlantic and Pacific SST are strongly anti-correlated with those of SST during summer (Figs. 3a, 4a). EIS is a measure of the strength of the temperature inversion capping the MBL, and a strong inversion has been shown to enhance subtropical low cloudiness by reducing entrainment drying of the MBL (Klein and Hartmann 1993; Wood 2012; Myers and Norris 2013; Bretherton 2015). Therefore, EIS anomalies appear to reinforce the SW CRE and low + mid-level CF anomaly patterns, while those in other cloud-controlling factors are not coherently related to either SST or SW CRE (Figs. 3b–d, 4b–d). These inferences are further confirmed by examination of the summertime pattern correlation coefficients among the SW CRE and cloud-controlling factor regression slopes over the North Atlantic (10–60°N, 80–0°W) and Pacific (10–60°N, 120–260°E) (Tables S2

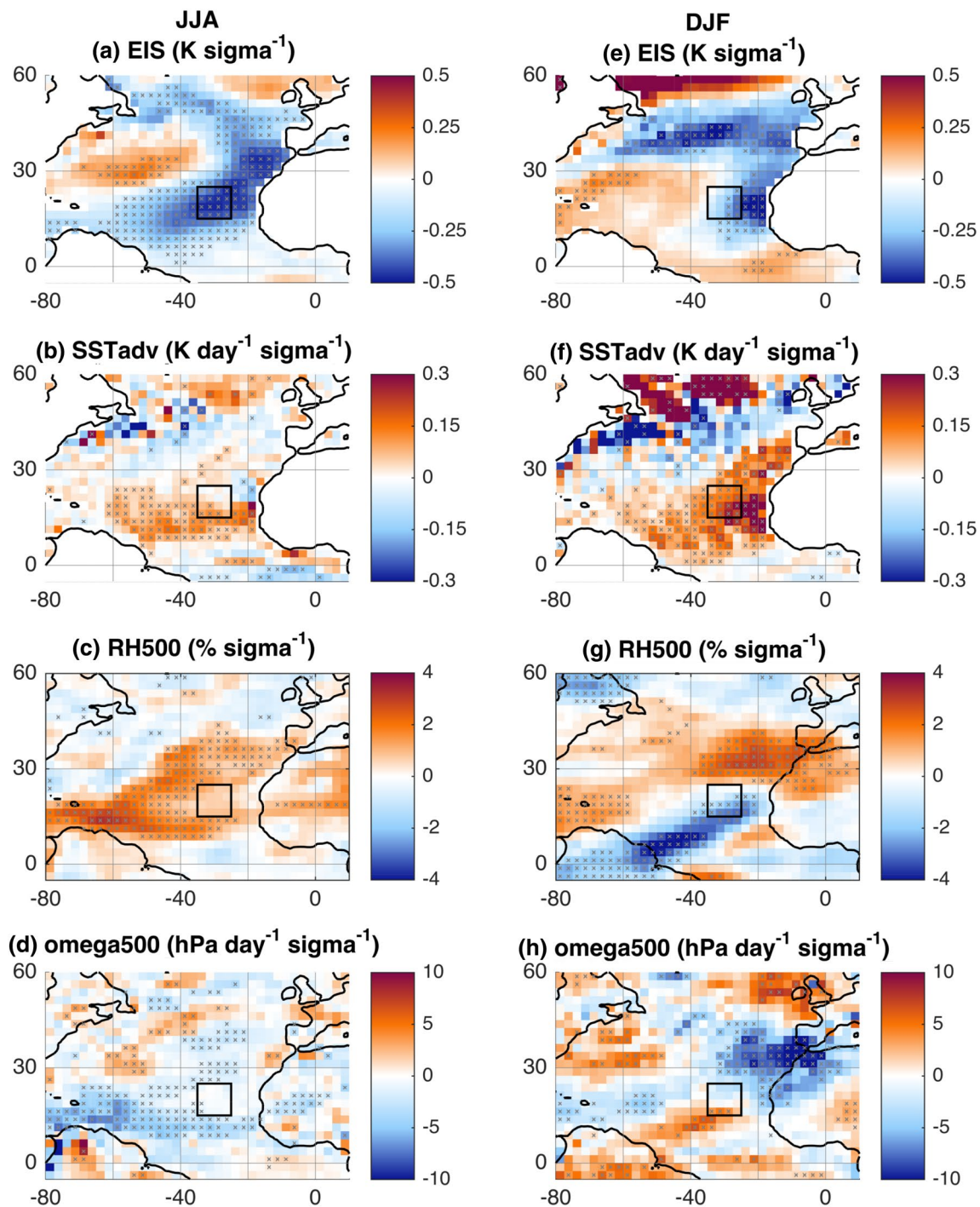


Fig. 3 As in Fig. 1 but for regression of JJA **a** EIS, **b** SSTadv, **c** RH₅₀₀, and **d** ω_{500} anomalies onto the 1985–2014 normalized time series of JJA SST anomalies averaged over the subtropical NE Atlantic. **e–h** are as in **a–d** but for DJF

and S3). Hence, typical summertime anomalies of SST and EIS over the subtropical and midlatitude northern oceans are the primarily meteorological factors related to basin-scale anomalies in SW CRE.

The right panels of Figs. 1 and 2 show the results corresponding to the left panels, but for DJF. Again, nearly

identical patterns emerge when the fields are regressed onto the normalized time series of the first PC of the EOF of North Atlantic or Pacific DJF SST anomalies, each of which exhibits substantial interannual and interdecadal variability. Wintertime SW CRE anomalies associated with a standard deviation increase in SST over the

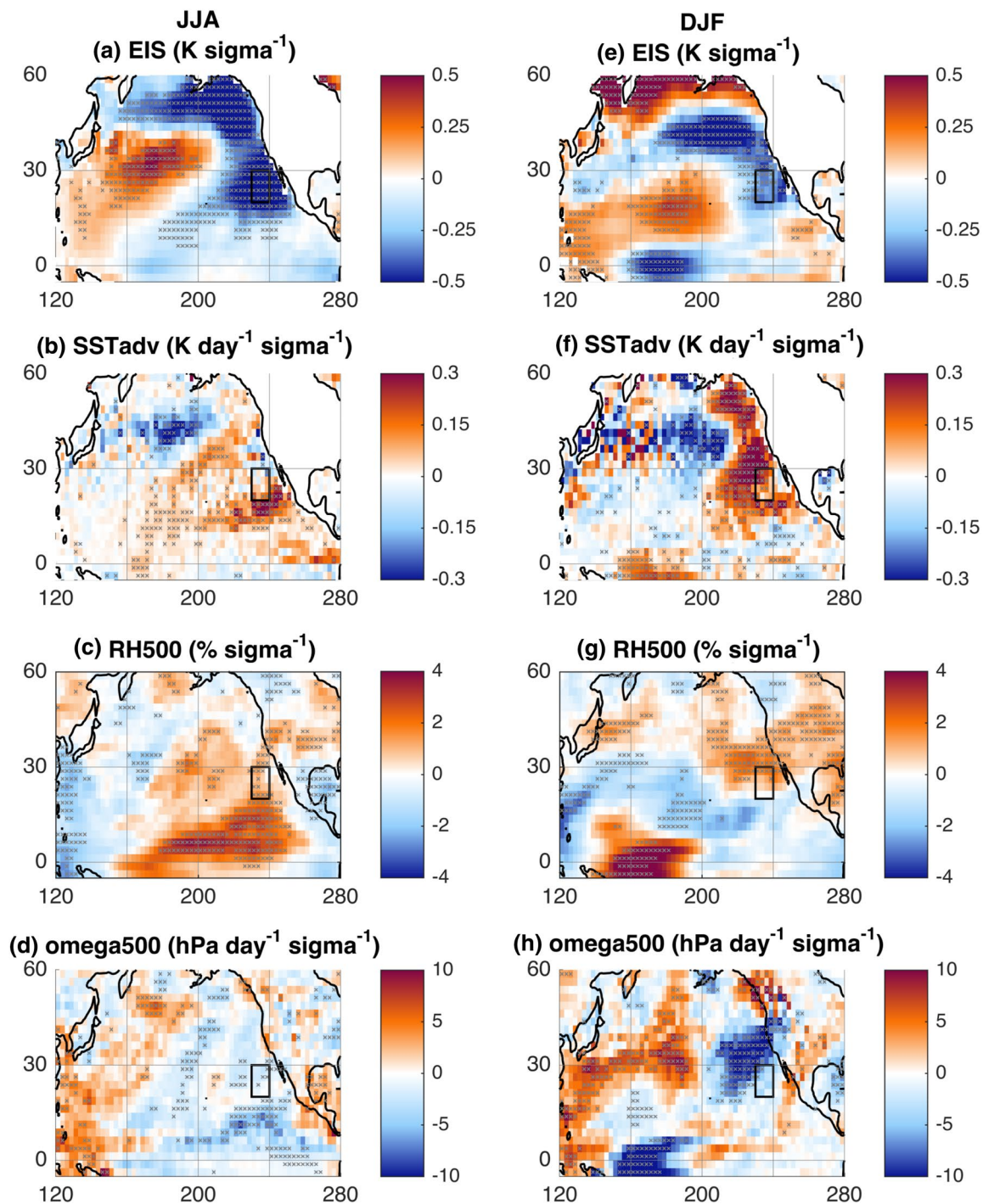


Fig. 4 As in Fig. 1 but for regression of JJA **a** EIS, **b** SSTadv, **c** RH₅₀₀, and **d** ω_{500} anomalies onto the 1985–2014 normalized time series of JJA SST anomalies averaged over the subtropical NE Pacific. **e–h** are as in **a–d** but for DJF

subtropical NE Atlantic and Pacific are consistent with a positive cloud feedback over the subtropics, especially southwest of the boxed regions of maximum stratiform cloud amount (Figs. 1d–e, 2d–e). Over the midlatitude North Atlantic SW CRE anomalies are much weaker than they are in summer yet also indicative a positive cloud

feedback, while over the midlatitude North Pacific weak SW CRE anomalies are not coherently co-located with SST anomalies. These patterns of SW CRE anomalies also emerge in surface net CRE and total CF and reflect changes in both low + mid- and high-level CF (Figs. S1–S4). Over the midlatitude North Atlantic, total CF

anomalies have similar magnitudes as they do in summer yet those of SW CRE are weaker in winter, indicating that reduced incident solar radiation at TOA during winter dampens the radiative impact of changes in cloudiness relative to summer. Over the midlatitude North Pacific, total CF anomalies have weaker magnitudes in winter than they do in summer due to substantial offset between low + mid- and high-level CF anomalies, explaining why those of SW CRE are also much weaker in winter. We note that the North Atlantic SST anomaly pattern during winter (Fig. 1e) is similar to that during summer, but features more of a tripole-like than horseshoe-like structure wherein cool SST in the central North Atlantic extends across almost the entire the basin and is flanked meridionally by warm SST. The North Pacific SST anomaly pattern during winter closely resembles that during summer (Fig. 2e). SLP and surface wind anomalies associated with wintertime SST variability (Figs. 1f, 2f) are substantial. NAO-like and Pacific North American (PNA)-like patterns of atmospheric circulation are evident, featuring anomalous midlatitude low-pressure centers over the North Atlantic and Pacific. These atmospheric conditions may force the observed patterns of extratropical (north of $\sim 10^\circ\text{N}$ including the subtropics and midlatitudes) SST anomalies by modifying surface sensible and latent heat fluxes (Cayan 1992; Deser and Blackmon 1993; Saravanan 1998; Alexander 2010; Fan and Schneider 2012). During summer, the NAO and PNA patterns are suppressed yet SST anomalies of comparable magnitude as those during winter occur, suggesting that the co-located anomalies of SW CRE play a role in the observed amplitude of the SST patterns. We acknowledge that the persistence of wintertime-generated SST anomalies can also contribute to the SST anomalies observed in summer (e.g. Vimont et al. 2001), although this does not preclude the role of a positive cloud feedback.

Regression slopes of other cloud-influencing factors onto subtropical NE Atlantic and Pacific SST during winter are shown in the right panels of Figs. 3 and 4. The anti-correlation between SST and EIS anomalies that occurs during summer is absent during winter, likely due to substantial changes in free-tropospheric temperature associated with the NAO and PNA patterns (Figs. 3e, 4e). SSTadv, RH₅₀₀, and ω_{500} anomalies per standard deviation increase in subtropical NE Atlantic and Pacific SST are much larger than they are in summer due to the substantial changes in atmospheric circulation (Figs. 3f–h, 4f–h). Hence, the pattern of SW CRE anomalies over the northern oceans during winter is driven by a combination of changes in several cloud-controlling factors, minimizing the basin-scale coherence between cloudiness, SST, and EIS that is so prominent in summer. This is reflected in the wintertime pattern correlation coefficients among the SW CRE and cloud-controlling

factor regression slopes over the North Atlantic and Pacific, which also show a large role for RH₅₀₀ in shaping the SW CRE anomalies during winter (Tables S4 and S5).

It is important to note that, while not identical, the fundamental patterns of SW CRE, SST, SLP, and surface winds associated with a standard deviation increase in subtropical NE Atlantic and Pacific SST are reproduced using either 1985–2000 (when ISCCP satellite cloud data is available) or 2001–2014 (when CERES satellite cloud data is available) interannual anomalies, indicating that the results are robust to time period and satellite cloud dataset (Figs. S5–S8). During either time period, the enhanced basin-scale cloud-SST and cloud-EIS coupling and reduced SLP variability during summer relative to winter over each ocean basin is evident. The effect of using the 1985–2014 combined record of anomalies to compute the regression slopes (Figs. 1, 2) is essentially to produce averages of the regression slopes from the separate time periods and to increase sample size.

3.2 Link between cloud feedback and summertime SST variability in CMIP5 models

On average, do CMIP5 models reproduce these observed patterns of variability over the northern oceans? Regression patterns as those in Figs. 1 and 2 for individual models can differ greatly from each other, which will be clear in the results below. Does this reflect discrepancies in their simulation of the cloud-SST feedback? To address this question, for each model we quantify the feedback between subtropical MBL clouds and SST by regressing the time series of detrended monthly anomalies (for all calendar months) of SW CRE averaged over each subtropical MBL cloud region onto similarly averaged SST anomalies. Only months for which ω_{500} exceeds 10 hPa day⁻¹ are used in the calculation to ensure that the resulting regression slope, SW/SST, is associated with processes associated with MBL clouds. All calendar months are used in the calculation in order to increase sample size and to approximate the inherent relationship between SST and SW CRE that is likely uniquely determined by each model's cloud and turbulence parameterization schemes (Qu et al. 2014). SW/SST is a bulk metric of the subtropical MBL cloud-SST feedback that reflects: (1) the effect of SST on the clouds; (2) the effect of the strength of the temperature inversion on the clouds, since SST and inversion strength are negatively correlated (e.g. Qu et al. 2014; Myers and Norris 2015); (3) the effect of any other cloud-controlling factor that is correlated to SST (e.g. free-tropospheric humidity) on the clouds; and (4) the radiative effect of the clouds on SST itself. Next, for each subtropical cloud region we partition models into three subsets according to their values of the SW/SST slope. The seven models with the highest values and the

seven models with the lowest values comprise the models with strong and weak feedbacks, respectively. The remaining subset comprises models with intermediate slope values (moderate feedback).

In Fig. 5 we plot the respective averages of the summertime North Atlantic regression patterns associated with a standard deviation increase in subtropical NE Atlantic SST for models with a weak MBL cloud-SST feedback in this region and for those with a strong feedback. X's indicate where the difference between the two subsets is statistically significant at the 90% confidence level, based on a two-tailed t test. Throughout the basin in the subtropics and midlatitudes, models with a weak feedback produce much smaller and less realistic positive SW CRE anomalies (Fig. 5a) than those produced by models with a strong feedback (Fig. 5c) for a standard deviation increase in SST over the subtropical NE Atlantic. This indicates that the SW/SST slope is related to cloud processes not only over the subtropical NE Atlantic, but over other regions as well. These include the midlatitudes where stratus and stratocumulus clouds are prevalent and the subtropics toward the equator where trade cumulus clouds are prevalent. The difference

in the amplitude of the SW CRE pattern between the two subsets of models also suggests that the discrepancy in the SW/SST slope is sufficient to explain the changes in cloudiness between the subsets. It is also evident that models with a weak cloud/SST feedback produce smaller and less realistic positive SST anomalies (Fig. 5b) than those produced by models with a strong feedback (Fig. 5d). This suggests a role for clouds in summer-to-summer SST variability over the North Atlantic. During winter, differences in the extratropical SW CRE and SST regression patterns between the two subsets of models (not shown) are more minor and generally not statistically significant for the SST difference, indicating a diminished role of clouds in North Atlantic SST variability during the season when the NAO pattern develops.

To more clearly discern reasons for the differences in SW CRE and SST among the models, in Fig. 6a we plot the subtropical NE Atlantic SW/SST slope against the local amplitude of SW CRE per standard deviation increase in subtropical NE Atlantic summertime SST for all models and observations. The SW CRE amplitude is defined as the regression value averaged over the subtropical NE Atlantic

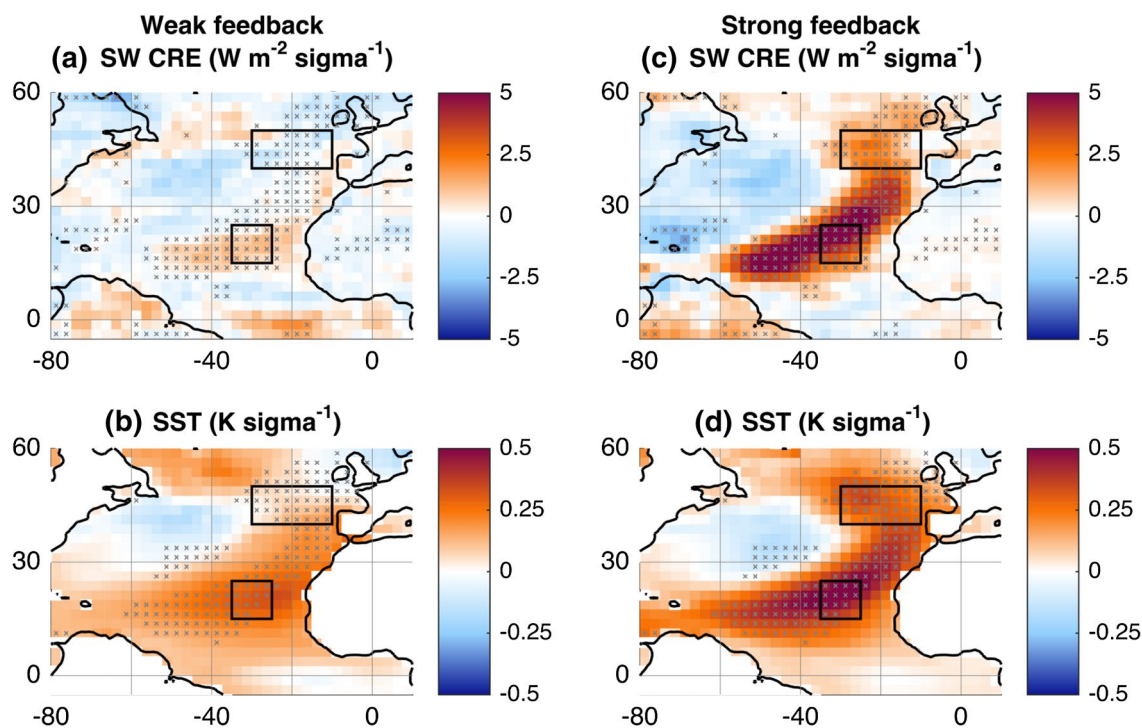


Fig. 5 Mean of slopes of regression of JJA **a** SW CRE at TOA and **b** SST anomalies onto the 1976–2005 normalized time series of JJA SST anomalies averaged over the subtropical NE Atlantic based on historical runs for CMIP5 models with a weak MBL cloud-SST feedback. **c** and **d** are as in **a** and **b** but for models with a strong cloud-SST feedback. Models have a weak (strong) cloud-SST feedback if they are among those with the seven lowest (highest) values of the

slope of the regression of the time series of monthly anomalies of SW CRE averaged over the subtropical NE Atlantic onto similarly averaged SST anomalies. X's indicate where the difference between the two subsets is statistically significant at the 90% confidence level using a two-tailed t test. The region in the midlatitude NE Atlantic used to compute the SST and SW CRE amplitudes listed in Table 1 is outlined with a *black rectangle*

stratiform cloud region, e.g. the average over the black rectangle of the pattern shown in Fig. 1a for 1985–2014 observations (merged obs.). Models are color-coded according to the subset of SW/SST feedback strength they reside in. The SW CRE amplitude per standard deviation warming is approximately equal to SW/SST times the standard deviation of JJA SST, so the SW CRE amplitude is related to SW/SST and the amount of typical SST warming itself. Figure 6a shows that the SW CRE amplitude per standard deviation warming is positively correlated with SW/SST ($r=0.78$, including merged obs. only), showing that differences in this quantity among models and observations can explain most of the differences in SW CRE independent of differences in the amount of typical SST warming. Figure 6b shows the subtropical NE Atlantic SW CRE amplitude plotted against the similarly defined SST amplitude. Note that the latter is almost identical to the summer-to-summer standard deviation in subtropical NE Atlantic SST. SW CRE amplitude is positively correlated with that of SST ($r=0.68$), and models with a strong MBL cloud feedback generally produce higher and more realistic SW CRE and SST amplitudes per standard deviation warming compared to models with a weak feedback. This suggests that differences in SW CRE per standard deviation warming, linked to unique SW/SST slopes, produce differences in SST by altering the surface radiation balance. Lastly, Fig. 6c shows SW/SST plotted against the subtropical NE Atlantic SST amplitude. Generally, as SW/SST increases, so too does the SST amplitude ($r=0.48$, and $r=0.68$ if outlier model IPSL-CM5B-LR is excluded).

To corroborate these results, we next consider a simple model of the energy balance of the ocean mixed layer. The sensitivity of SST to the surface heat flux F into the mixed layer can be approximated as (Cronin et al. 2013)

$$\frac{\Delta \text{SST}}{\Delta F} = \frac{\Delta t}{\rho c_p z}$$

where ρ is the density of seawater, c_p is the specific heat of seawater at constant pressure, z is the depth of the mixed layer, and Δt is the time interval. Using the average of density- and temperature-based climatological mean z during JJA for the subtropical NE Atlantic box based on the dataset produced by de Boyer Montégut et al. (2004), we obtain $z=35$ m (this dataset is also used for all subsequent values of z). Thus, for $\rho=1025$ kg m⁻³, $c_p=3994$ J kg⁻¹ K⁻¹, and $\Delta t=90$ days (the approximate number of days in a 3-month season), we find that $\Delta \text{SST}/\Delta F=0.05$ K/(W m⁻²). This value is quantitatively similar to the slope of the linear regression fit (including merged obs. only) between the SW CRE and SST amplitudes shown in Fig. 6b, which is 0.04 ± 0.03 K/(W m⁻²), where uncertainty indicates 95% confidence bounds. Also, for the midlatitude NE Atlantic (outlined with a black rectangle in Fig. 5), $z=20$ m, so

we estimate that $\Delta \text{SST}/\Delta F=0.1$ K/(W m⁻²). This value is quantitatively similar to the slope of the fit between the SW CRE and SST amplitudes averaged over the midlatitude NE Atlantic, which is 0.08 ± 0.04 K/(W m⁻²). The comparison between the regression slopes and $\Delta \text{SST}/\Delta F$ is justified because simulations and observations provide several possible realizations of climate anomalies for 3-month seasonal averages, so variations in the SW CRE and SST amplitudes can be considered to be analogous to seasonally averaged variations in surface heat flux and the resulting change in SST. The close alignment of the regression slopes and $\Delta \text{SST}/\Delta F$ suggests that cloud variations can alter the surface energy balance sufficiently to force differences in SST in the North Atlantic. For a given amount of warming over the North Atlantic, models simulate large differences in cloudiness that contribute to inter-model differences in the amount of typical warming itself by a positive cloud feedback.

Do clouds also play an important role in disparities of North Pacific atmosphere–ocean variability among climate models? In Fig. 7 we plot the respective averages of the summertime North Pacific regression patterns associated with a standard deviation increase in subtropical NE Pacific SST for models with a weak MBL cloud–SST feedback in this region and for those with a strong feedback. Throughout the NE Pacific, models with a weak feedback produce smaller and less realistic SW CRE (Fig. 7a) and SST anomalies (Fig. 7b) than those with a strong feedback (Fig. 7c, d) for a standard deviation increase in SST over the subtropical NE Pacific. This suggests a role for clouds in summer-to-summer SST variability over the North Pacific. During winter, differences in the extratropical SW CRE and SST regression patterns between the two subsets of models (not shown) are more minor and generally not statistically significant for the SST difference, indicating a diminished role of clouds in North Pacific SST variability during the season when the PNA pattern develops. Figure 7c, d also show that, interestingly, models with a weak SW/SST feedback unrealistically produce small negative anomalies of SST in the eastern tropical Pacific, while models with a strong feedback realistically produce small positive anomalies. Examination of the SLP and surface wind regression patterns (not shown) indicates that this difference is linked to a weakening of the climatological easterlies and zonal SLP gradient along the equator in models with a strong SW/SST feedback. Hence, it is plausible that the SW/SST slope captures key processes involved in the El Niño–Southern Oscillation (ENSO), such as the transition between stratiform and convective cloudiness that occurs over the eastern equatorial Pacific. However, this inference is tenuous based on our results and the role of clouds in ENSO requires further analysis.

Table 1 NE Atlantic SW/SST slope and SW CRE and SST amplitudes per standard deviation increase in subtropical NE Atlantic summertime SST in models with weak, moderate, and strong MBL cloud-SST feedbacks and observations

	Weak	Moderate	Strong	Observations
Subtropical SW/SST slope ($\text{W m}^{-2} \text{K}^{-1}$)	0.92	4.3	8.2	6.7 ± 2.7
Subtropical SW CRE amp ($\text{W m}^{-2} \text{sigma}^{-1}$)	0.78	2.1	4.4 ($p=0.00$)	4/4.8/3.1
Subtropical SST amp (K sigma^{-1})	0.3	0.41	0.46 ($p=0.04$)	0.44/0.49/0.39
Midlatitude SW CRE amp ($\text{W m}^{-2} \text{sigma}^{-1}$)	-0.49	0.29	1.6 ($p=0.02$)	1.9/2/1.8
Midlatitude SST amp (K sigma^{-1})	0.07	0.08	0.29 ($p=0.02$)	0.32/0.46/0.14

p values are based on a two-tailed t test of the difference in SW CRE or SST amplitude between the weak and strong subsets of models. The observed SW/SST slope is for 1985–2014 observations and shows a 95% confidence interval. Each observed amplitude from left to right is based on 1985–2014, 1985–2000, and 2001–2014 observations

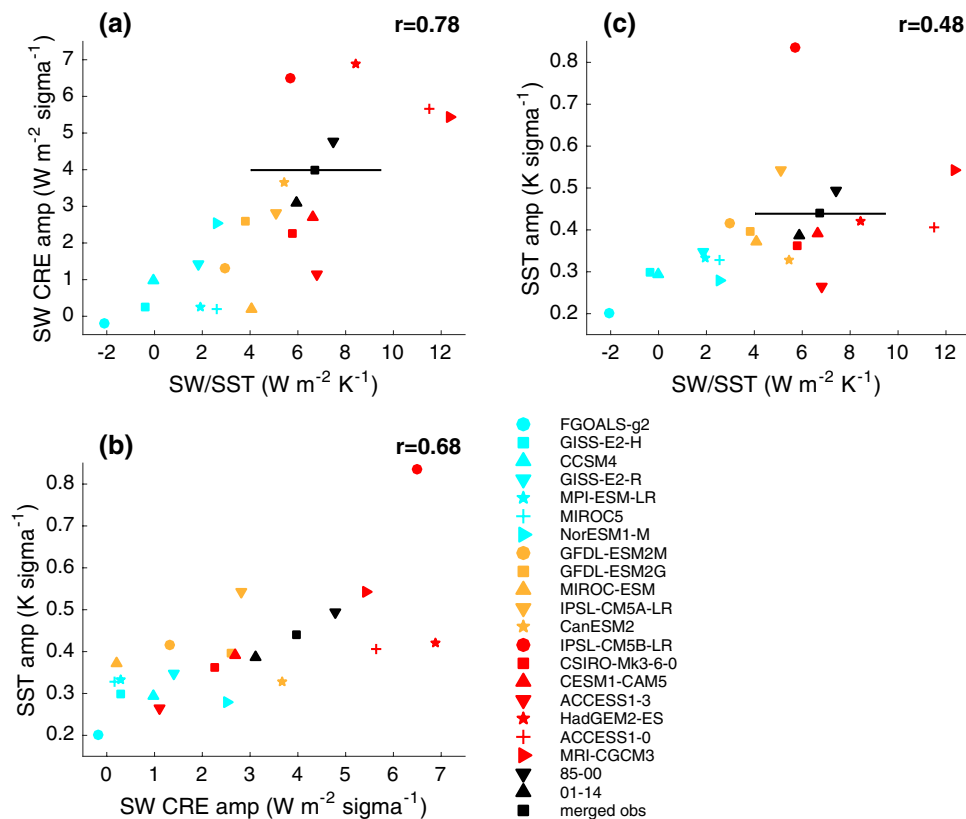


Fig. 6 Relationships among the subtropical NE Atlantic MBL cloud-SST feedback parameter and the local SW CRE and SST amplitudes per standard deviation increase in subtropical NE Atlantic summertime SST. The SW CRE and SST amplitudes are defined as their respective regression values averaged over the subtropical NE Atlantic stratiform cloud region, e.g. the averages over the *black rectangle* of the patterns shown in Fig. 1a, b for 1985–2014 observations (merged obs). **a** SW/SST slope plotted against SW CRE amplitude,

b SW CRE amplitude plotted against SST amplitude, and **c** SW/SST slope plotted against SST amplitude. The error bars for the SW/SST slope computed using 1985–2014 data (merged obs) denote 95% confidence bounds, taking into account temporal autocorrelation. *Cyan, orange, and red symbols* denote models with weak, moderate, and strong subtropical NE Atlantic MBL cloud-SST feedbacks. Models in the legend are listed *from top to bottom* in increasing order of their feedback strength. Observations are in *black*

Figure 8a shows the subtropical NE Pacific SW/SST slope plotted against the local amplitude of SW CRE associated with a standard deviation increase in subtropical NE Pacific summertime SST for all models and observations. The SW CRE amplitude is defined as the SW CRE regression value averaged over the subtropical NE Pacific

stratiform cloud region. SW CRE amplitude is positively correlated with SW/SST ($r=0.80$), indicating that differences in SW/SST among models and observations are primarily what drive differences in the amplitude of SW CRE. Figure 8b shows the subtropical NE Pacific SW CRE amplitude plotted against the similarly defined SST

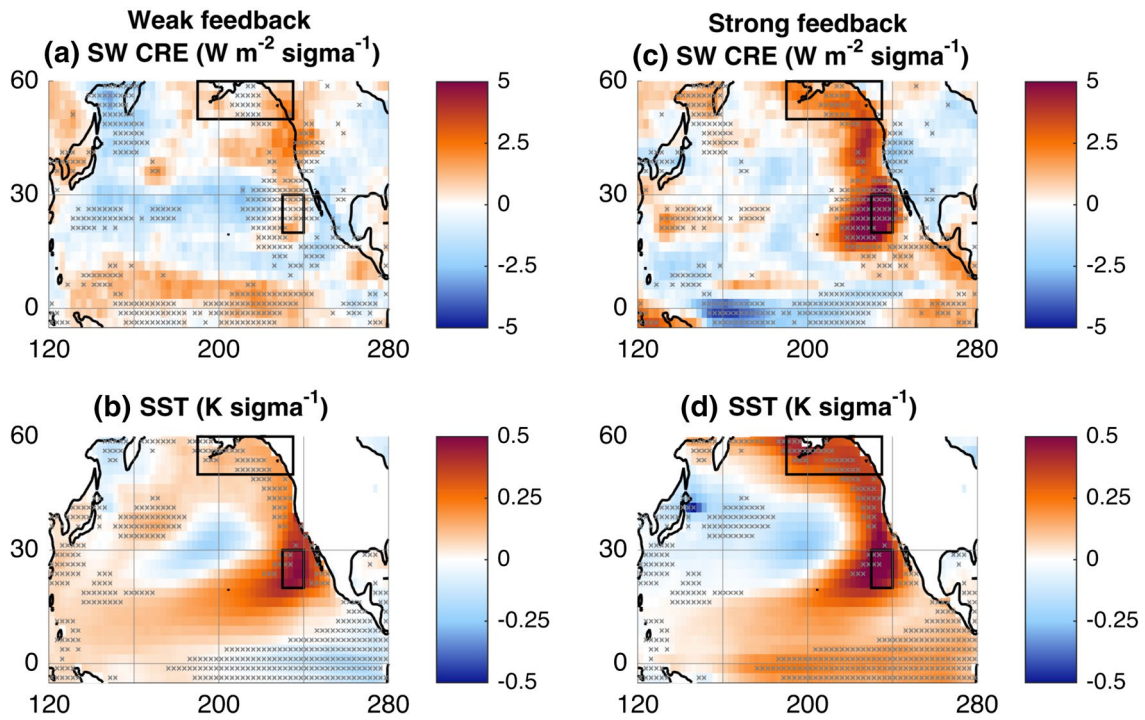
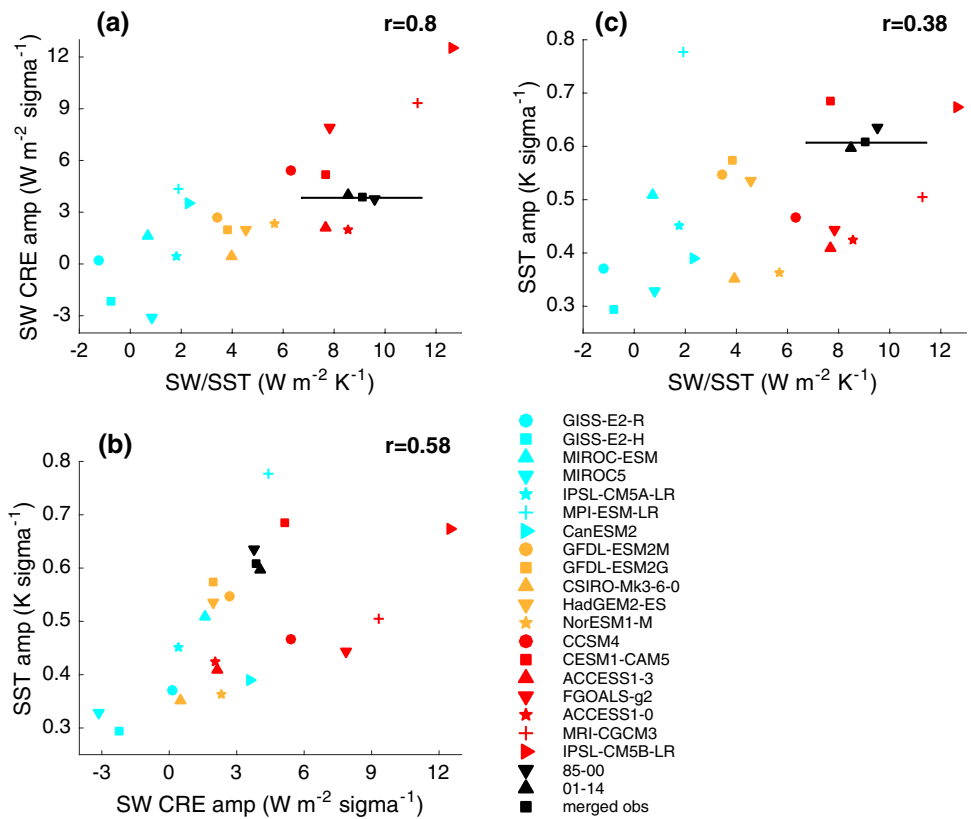


Fig. 7 As in Fig. 5 but for the Pacific

Fig. 8 As in Fig. 6 but for the subtropical NE Pacific



amplitude. SW CRE amplitude is positively correlated with that of SST ($r=0.58$), suggesting that differences in SW CRE produce differences in SST. The slope of the linear regression fit between the subtropical SW CRE and SST amplitudes shown in Fig. 8b is 0.02 ± 0.01 K/(W m⁻²), while that between the amplitudes averaged over the midlatitude NE Pacific (outlined with a black rectangle in Fig. 7) is 0.12 ± 0.08 K/(W m⁻²). Such estimates are quantitatively similar to the values of $\Delta\text{SST}/\Delta F$ of 0.07 K/(W m⁻²) and 0.11 K/(W m⁻²) for $z=29$ m and $z=17$ m, respectively. These results further contribute to establish confidence in our physical interpretation that cloud variations may force differences in SST in the North Pacific by altering the surface energy balance. Lastly, Fig. 8c shows SW/SST plotted against the subtropical NE Pacific SST amplitude. Generally, as SW/SST increases, so too does the SST amplitude ($r=0.38$, and $r=0.57$ if outlier model MPI-ESM-LR is excluded). The qualitative similarity of the results for the two separate ocean basins provides support for the notion that MBL clouds can amplify climate modes of variability.

Tables 1 and 2 summarize the role of clouds in summertime North Atlantic and Pacific SST variability. Table 1 lists averages of the subtropical NE Atlantic SW/SST slope as well as averages of the subtropical and midlatitude NE Atlantic SW CRE and SST amplitudes, per standard deviation increase in subtropical NE Atlantic SST, for the three subsets of models and observations. Table 2 lists averages for the Pacific. For both ocean basins, models with a strong SW/SST feedback simulate higher average amplitudes of subtropical and midlatitude SW CRE and SST than those of models with a weak feedback. Each difference is statistically significant except that of the subtropical NE Pacific SST amplitude, although we note that this is clearly influenced by the outlier model MPI-ESM-LR as seen in Fig. 8. Furthermore, the observed values of SW/SST, SW CRE amplitude, and SST amplitude are more similar to the average values of models with a strong subtropical SW/SST feedback than to those of models with a weak feedback (note that the averages of the 1985–2000 and 2001–2014 values are very similar to the values computed using the entire merged 1985–2014 record). The amplitude of summertime SST variability over the northern oceans in

CMIP5 models therefore appears to be sensitive to their simulation of the boundary layer cloud-SST feedback.

4 Conclusions

In this study, we investigate the satellite cloud record and CMIP5 models to determine whether MBL clouds can amplify modes of climate variability over the extratropical northern oceans. Over each ocean basin during summer, a standard deviation increase in subtropical SST resembles the dominant mode of SST variability and is associated with a horseshoe pattern of co-located anomalies of SW CRE, low + mid-level CF, SST, and EIS over the subtropics and midlatitudes that are consistent with MBL clouds' acting as a positive feedback on SST. The SST patterns over the North Atlantic and Pacific resemble those associated with the AMO and PDO. During winter, SST anomalies associated with a standard deviation increase in subtropical SST for each basin feature a similar pattern, but they are weakly related to basin-scale SW CRE and EIS anomalies. In this season, SLP and surface wind anomalies associated with these modes resemble the NAO and PNA patterns of variability over the North Atlantic and Pacific, respectively, and are much stronger than those that occur during summer. Horizontal surface temperature advection, free-tropospheric humidity, and vertical velocity anomalies are also stronger in winter than they are in summer, minimizing the dominant role of cloud-SST and cloud-EIS coupling during summer. The similarity of the seasonality between dominant modes of SST variability over the North Atlantic and Pacific suggests that MBL clouds play an important role in atmosphere–ocean variability during summer. During this season, clouds may make a substantial contribution to the surface energy budget because turbulent heat flux anomalies are weaker and the ocean mixed layer is shallower than they are during winter. This corroborates Norris et al. (1998), who performed a similar observational analysis for the North Pacific using different cloud observations and statistical methods.

There are large model-to-model differences in CMIP5 models' simulation of these patterns of variability. To investigate reasons for the inter-model spread of SW CRE and SST amplitudes associated with standard

Table 2 As in Table 1 but for the Pacific

	Weak	Moderate	Strong	Observations
Subtropical SW/SST slope (W m ⁻² K ⁻¹)	0.79	4.3	8.9	9.1 ± 2.4
Subtropical SW CRE amp (W m ⁻² sigma ⁻¹)	0.69	1.9	6.3 ($p=0.01$)	3.8/3.8/4
Subtropical SST amp (K sigma ⁻¹)	0.45	0.47	0.52 ($p=0.37$)	0.61/0.64/0.6
Midlatitude SW CRE amp (W m ⁻² sigma ⁻¹)	0.46	1.3	2.1 ($p=0.05$)	2.6/3.4/1.8
Midlatitude SST amp (K sigma ⁻¹)	0.11	0.25	0.35 ($p=0.06$)	0.45/0.39/0.54

deviation increases in subtropical NE Atlantic and Pacific SST during summer, we partition models according to the strength of the subtropical NE Atlantic and Pacific MBL cloud-SST feedback they simulate. The slope of the regression of SW CRE onto SST over the regions of maximum stratiform cloud amount identified by Klein and Hartmann (1993) serves as the metric of feedback strength. Models that simulate a strong cloud-SST feedback over the subtropical NE Atlantic and Pacific generally produce higher and more realistic typical amplitudes of SW CRE and SST variability over the subtropics and midlatitudes than those produced by models with a weaker feedback. Moreover, for the Atlantic and Pacific, the change in SST amplitude per unit change in SW CRE amplitude among the models and observations is similar to the temperature response of the ocean mixed layer to a unit change in radiative flux over the course of a season. These results strongly suggest that the amplitude of summer-to-summer SST variability over the northern oceans in coupled climate models is sensitive to their representation of MBL clouds. More specifically, they suggest that where MBL clouds are climatologically prevalent, they act to amplify the dominant modes of SST variability over the northern oceans during summer. These results are consistent with and bolster the findings of recent idealized modeling studies that show a substantial role of low clouds in unforced modes of climate variability (Evan et al. 2013; Bellomo et al. 2014, 2015, 2016; Brown et al. 2016). The substantial differences in the SW CRE and SST amplitudes of variability between models with weak and strong cloud/SST feedbacks do not occur in winter. Hence, the role of clouds in extratropical atmosphere–ocean variability over the northern oceans during this season is muted, as could be expected from the distinct physics underlying this variability during the season when the NAO and PNA patterns develop.

It is well known that improving the representation of MBL clouds in climate models will improve the simulation of mean climate and the reliability of anthropogenic warming projections. The results of the present study suggest that such an improvement may also lead to more realistic simulation of interannual to interdecadal summertime atmosphere–ocean variability over the extratropics.

Acknowledgements This study was funded by NOAA's Climate Program Office, Climate Variability and Predictability Program Award NA14OAR4310278. The research was partly carried out at the Jet Propulsion Laboratory, California Institute of Technology, under a contract with NASA. CERES data were obtained from the NASA Langley Research Center CERES ordering tool at <http://ceres.larc.nasa.gov/>. ISCCP data were downloaded from the Atmospheric Science Data Center located at NASA Langley Research Center. Joel Norris kindly provided the corrected ISCCP data. ERA-Interim data were downloaded from the ECMWF data server at <http://apps.ecmwf.int/datasets/>. The authors thank both the World Climate Research

Programme Working Group on Coupled Modeling, which is responsible for CMIP, and the climate modeling groups for producing and making available their model output. Lastly, the authors thank three anonymous reviewers for their thoughtful comments that led to improvements in the manuscript.

References

- Alexander M (2010) Extratropical air–sea interaction, sea surface temperature variability, and the Pacific Decadal Oscillation. *Climate dynamics: why does climate vary?* pp 123–148
- Bellomo K, Clement A, Mauritsen T, Rädcl G, Stevens B (2014) Simulating the role of subtropical stratocumulus clouds in driving Pacific climate variability. *J Clim* 27(13):5119–5131
- Bellomo K, Clement AC, Mauritsen T, Rädcl G, Stevens B (2015) The influence of cloud feedbacks on equatorial Atlantic variability. *J Clim* 28(7):2725–2744
- Bellomo K, Clement AC, Murphy LN, Polvani LM, Cane MA (2016) New observational evidence for a positive cloud feedback that amplifies the Atlantic Multidecadal Oscillation. *Geophys Res Lett* 43(18):9852–9859
- Bony S, Dufresne J (2005) Marine boundary layer clouds at the heart of tropical cloud feedback uncertainties in climate models. *Geophys Res Lett* 32(20):L20806
- Bretherton CS (2015) Insights into low-latitude cloud feedbacks from high-resolution models. *Phil Trans R Soc A* 373(2054):20,140,415
- Brown PT, Lozier MS, Zhang R, Li W (2016) The necessity of cloud feedback for a basin-scale Atlantic Multidecadal Oscillation. *Geophys Res Lett* 43(8):3955–3963
- Burgman R, Clement AC, Mitas C, Chen J, Esslinger K (2008) Evidence for atmospheric variability over the Pacific on decadal timescales. *Geophys Res Lett* 35(1):L01704
- Cassou C, Deser C, Terray L, Hurrell JW, Drévillon M (2004) Summer sea surface temperature conditions in the north Atlantic and their impact upon the atmospheric circulation in early winter. *J Clim* 17(17):3349–3363
- Cayan DR (1992) Latent and sensible heat flux anomalies over the northern oceans: driving the sea surface temperature. *J Phys Oceanogr* 22(8):859–881
- Clement AC, Burgman R, Norris JR (2009) Observational and model evidence for positive low-level cloud feedback. *Science* 325(5939):460–464
- Cronin MF, Bond NA, Farrar JT et al (2013) Formation and erosion of the seasonal thermocline in the Kuroshio extension recirculation Gyre. *Deep sea research part II: topical studies. Oceanography* 85:62–74
- de Boyer Montégut C, Madec G, Fischer AS, Lazar A, Iudicone D (2004) Mixed layer depth over the global ocean: an examination of profile data and a profile-based climatology. *J Geophys Res* 109(C12)
- Dee D, Uppala S, Simmons A, Berrisford P, Poli P, Kobayashi S, Andrae U, Balmaseda M, Balsamo G, Bauer P et al (2011) The Era-Interim reanalysis: configuration and performance of the data assimilation system. *Q J R Meteorol Soc* 137(656):553–597
- Deser C, Blackmon ML (1993) Surface climate variations over the North Atlantic Ocean during winter: 1900–1989. *J Clim* 6(9):1743–1753
- Evan AT, Allen RJ, Bennartz R, Vimont DJ (2013) The modification of sea surface temperature anomaly linear damping time scales by stratocumulus clouds. *J Clim* 26(11):3619–3630

- Fan M, Schneider EK (2012) Observed decadal North Atlantic tri-pole SST variability. Part I: weather noise forcing and coupled response. *J Atmos Sci* 69(1):35–50
- Garay MJ, de Szoeke SP, Moroney CM (2008) Comparison of marine stratocumulus cloud top heights in the southeastern Pacific retrieved from satellites with coincident ship-based observations. *J Geophys Res* 113:D18. doi:[10.1029/2008JD009975](https://doi.org/10.1029/2008JD009975)
- Klein SA, Hartmann DL (1993) The seasonal cycle of low stratiform clouds. *J Clim* 6(8):1587–1606
- Loeb NG, Wielicki BA, Doelling DR, Smith GL, Keyes DF, Kato S, Manalo-Smith N, Wong T (2009) Toward optimal closure of the Earth's top-of-atmosphere radiation budget. *J Clim* 22(3):748–766
- Mantua NJ, Hare SR, Zhang Y, Wallace JM, Francis RC (1997) A Pacific interdecadal climate oscillation with impacts on salmon production. *Bull Am Meteorol Soc* 78(6):1069–1079
- Myers TA, Norris JR (2013) Observational evidence that enhanced subsidence reduces subtropical marine boundary layer cloudiness. *J Clim* 26(19):7507–7524
- Myers TA, Norris JR (2015) On the relationships between subtropical clouds and meteorology in observations and CMIP3 and CMIP5 models. *J Clim* 28(8):2945–2967
- Norris JR, Evan AT (2015) Empirical removal of artifacts from the ISCCP and PATMOS-x satellite cloud records. *J Atmos Ocean Technol* 32(4):691–702
- Norris JR, Zhang Y, Wallace JM (1998) Role of low clouds in summertime atmosphere–ocean interactions over the North Pacific. *J Clim* 11(10):2482–2490
- Qu X, Hall A, Klein SA, Caldwell PM (2014) On the spread of changes in marine low cloud cover in climate model simulations of the 21st century. *Clim Dyn* 42(9):2603–2626
- Reynolds RW, Rayner NA, Smith TM, Stokes DC, Wang W (2002) An improved in situ and satellite SST analysis for climate. *J Clim* 15(13):1609–1625
- Rossow WB, Schiffer RA (1999) Advances in understanding clouds from ISCCP. *Bull Am Meteorol Soc* 80(11):2261–2287
- Saravanan R (1998) Atmospheric low-frequency variability and its relationship to midlatitude SST variability: studies using the NCAR Climate System Model. *J Clim* 11(6):1386–1404
- Stephens GL, Li J, Wild M, Clayson CA, Loeb N, Kato S, L'Ecuyer T, Stackhouse PW Jr, Lebsock M, Andrews T (2012) An update on Earth's energy balance in light of the latest global observations. *Nat Geosci* 5(10):691–696
- Sun M, Doelling DR, Raju RI, Nguyen LC, Loeb NG (2010) The CERES ISCCP-D2like cloud and radiative property data product. AGU Fall Meeting Abstracts
- Tanimoto Y, Xie SP (2002) Inter-hemispheric decadal variations in SST, surface wind, heat flux and cloud cover over the Atlantic Ocean. *J Meteorol Soc Jpn* 80(5):1199–1219
- Taylor KE, Stouffer RJ, Meehl GA (2012) An overview of CMIP5 and the experiment design. *Bull Am Meteorol Soc* 93(4):485–498
- Vimont DJ, Battisti DS, Hirst AC (2001) Footprinting: a seasonal connection between the tropics and mid-latitudes. *Geophys Res Lett* 28(20):3923–3926
- Wang H, Kumar A, Wang W, Xue Y (2012) Seasonality of the Pacific Decadal Oscillation. *J Clim* 25(1):25–38
- Wood R (2012) Stratocumulus clouds. *Mon Weather Rev* 140(8):2373–2423
- Wood R, Bretherton CS (2006) On the relationship between stratiform low cloud cover and lower-tropospheric stability. *J Clim* 19(24):6425–6432
- Yuan T, Oreopoulos L, Zelinka M, Yu H, Norris JR, Chin M, Plattnick S, Meyer K (2016) Positive low cloud and dust feedbacks amplify tropical North Atlantic Multidecadal Oscillation. *Geophys Res Lett* 43(3):1349–1356
- Zhang Y, Rossow WB, Lacis AA, Oinas V, Mishchenko MI (2004) Calculation of radiative fluxes from the surface to top of atmosphere based on ISCCP and other global data sets: refinements of the radiative transfer model and the input data. *J Geophys Res* 109:D19105. doi:[10.1029/2003JD004457](https://doi.org/10.1029/2003JD004457)